J Solid State Electrochem (2011) 15:213–221
DOI 10.1007/s10008-010-1227-1

REVIEW

Controlling the proton transport properties of solid acids via structural and microstructural modification

Valentina Ponomareva · Galina Lavrova

Received: 5 October 2010 / Revised: 21 October 2010 / Accepted: 22 October 2010 / Published online: 20 November 2010

Abstract This survey deals with the problems of composite proton electrolytes based on superprotonic acid salts $M_mH_n(XO_4)_p$ (M=Cs, Rb, K, Na, Li, NH_4; A=S, Se, As, P), their transport, structural properties, and thermal stability. The main factors determining the composite properties are the type of oxide matrix, its morphology, surface acidity of the components, structural peculiarities of the salts, hydrogen bond network, and relative humidity. The review discusses briefly the synthesis and structures of these materials, as well as the influence of disordered states of the salt in composites on their unusual properties. The important role of hydrogen bonds for the interfacial interaction in the composite solid electrolytes is discussed.

Keywords Proton composite · Solid electrolyte · Solid acids · Silica

Introduction

Last decade, the scientific interest to the superionic acid salts, so-called "solid acids," is highly amplified because of their possible application in the fuel cells, which emerge as attractive alternatives to combustion engines. These compounds have significant advantages among proton-conducting solid electrolytes due to anhydrous proton transport at intermediate temperatures; new types of fuel cells, solid acid fuel cell, are now under intensive investigation [1–12].

Solid acids $M_mH_n(XO_4)_p$ (M=Cs, Rb, K, Na, Li, NH_4; A=S, Se, As, P) undergo a "superprotonic" phase transition at temperatures 50–230 °C accompanied by a sharp increase in the conductivity up to 10^{-3}–10^{-2} Scm^{-1} (Fig. 1). As a rule, superionic phases have cubic or tetragonal structure and dynamically disordered hydrogen bond networks [13–19], in which the number of equivalent positions in the crystal structure is several times larger than the proton concentration. The transport mechanism involves the fast rotations of XO_4 anions, which facilitate proton transfer from one anion to another and provide low activation energy of the conductivity (0.2–0.4 eV). At room temperature, solid acids have rather fixed hydrogen bond network with moderate and strong hydrogen bonds (6–14 $kcal\,mol^{-1}$). The peculiarities of hydrogen bond network and in particular, its dimension, determine a wide variety of structures (most often monoclinic or hexagonal), thermodynamic, and transport properties of the salts. Proton transport within the static hydrogen bond network occurs via the point defect migration with activation energy of 0.6–1.0 eV, and the conductivity usually does not exceed 10^{-8}–10^{-6} Scm^{-1}. The mechanical stresses at the temperatures close to superionic phase transition ($T_{ph.tr.}$) hamper practical application of the acid salts.

Since the discovery of the first solid acid, $CsHSO_4$ ($T_{ph.tr.}$=141 °C) attempts to improve the low-temperature (LT) conductivity of solid acids result in a continuous progress. First, Colomban et al. [20–22] had shown that the partial substitution of Cs^+ by Li^+, K^+, or Rb^+ induces weakening of hydrogen bonds in $CsHSO_4$ at room temperatures and, as a result, leads to more disordered state with enhanced conductivity. Similar effects were also observed in $Cs_mH_n((S,P)O_4)_p$ mixed salts, where some

This work is dedicated to Prof. R. Schöllhorn on his 75th birthday.

V. Ponomareva (✉) · G. Lavrova
Institute of Solid State Chemistry and Mechanochemistry,
Siberian Branch of Russian Academy of Sciences,
Kutateladze 18,
630128, Novosibirsk, Russia
e-mail: ponomareva@solid.nsc.ru

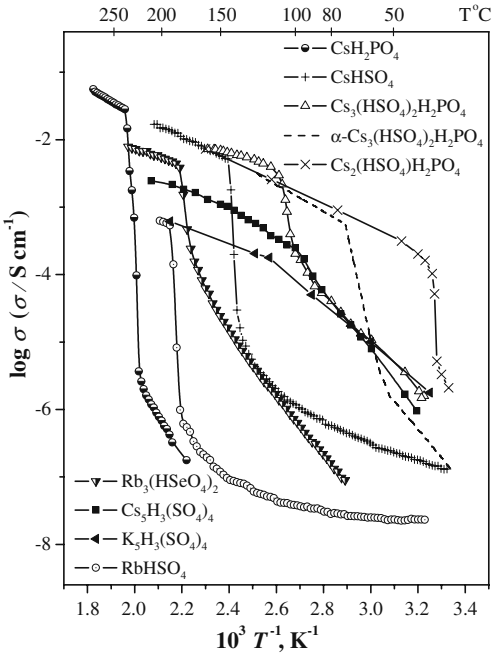

Fig. 1 Temperature dependencies of conductivity for some superprotonic acid salts

hydrogen bond network disordering takes place [23–26]. As a result, in these compounds the superionic phase transition temperature is lower and conductivity of LT phases is higher than those in both $CsHSO_4$ and CsH_2PO_4 (Fig. 1).

Another way to enhance the transport properties of the ionic salt together with improvement of its mechanical properties, as shown for the first time about 40 years ago [27], is the heterogeneous doping with highly dispersed oxides. Today, this method is widely used for upgrading different kind of ionic electrolytes, including proton conductors, such as zirconium phosphate, heteropolyacids, antimonic acid, iron and tantalum sulfate hydrates, ammonium polyphosphates [28–33], and different solid acids [34–48]. Actually, the state of salt and the degree of disordering in the composite differ markedly and depend on many factors. That is why the transport and thermodynamic properties of composites are so miscellaneous.

This paper presents a brief survey on our developments of proton composite electrolytes based on solid acids, especially, $CsHSO_4$ and CsH_2PO_4. Special attention is given to the factors determining the stabilization of different disordered phases, influence of salt structure on proton transport, and stability of materials.

Experimental

Crystals of the acid salts were grown from aqueous solutions of basic salt and acid (for example, Cs_2SO_4 and H_2SO_4) in the stoichiometric ratio at 25 °C. The synthesized salts have been identified by X-ray diffraction (XRD) and elemental analysis. For the composites preparation, various highly dispersed matrices were used, such as SiO_2 with different specific surface areas (S_{sp}=13–580 m^2g^{-1}) and a uniform pore-size distribution, TiO_2 (S_{sp}=100, 480 m^2g^{-1}), Al_2O_3 (S_{sp}=70, 270 m^2g^{-1}), and SiP_2O_7 (S_{sp}=11 m^2g^{-1}). Silica phosphate gels with different Si/P ratio (1: 0.25 to 1: 0.07, S_{sp}=3.8, 520 m^2g^{-1}) obtained by sol–gel method were also used to prepare composites. Specific surface areas of matrices, pore volume (V_{por}), and pore size (r_{por}) distribution were determined by the BET method. The mole fraction of dopant A, x, in $(1-x)$ $M_mH_n(XO_4)_p$–xA composites varied from 0.1 to 0.95. The components were carefully grinded and mixed in agate mortar and then pressed at 500 MPa to form a pellet. The relative density of the samples was 90–95%. The prepared pellets were heated in air at 205–245 °C for 20 min.

The conductivity was measured using a Hewlett-Packard 4284A Precision LCR-meter and Instek LCR 821 m over the frequency range 5 Hz–1 MHz using an Ag- or Pt-pressed electrodes in a cooling regime with the rate of 2–3 °C min^{-1} in air with different humidity values (0.6–30 mol% H_2O). The XRD analysis was performed using a DRON-3 Diffractometer with monochromatic CuK_α radiation at room temperature. Thermogravimetric analysis and differential scanning calorimetry (DSC) were performed with a Jupiter NETZSCH STA 449C instrument and DSC-550 ISI from 20 °C to 400 °C at a heating rate of 5–10 °C min^{-1} and a gas (He or air) flow rate of 2 ml min^{-1}. Infrared spectra were obtained using a DIGILAB EXCALIBUR 3100 ATR (ZnSe) and BOMEM MB-102 Fourier spectrometers in the frequency ranges 4,000–400 cm^{-1} at room temperature. The materials were powdered and measured in a mineral oil. Raman spectra were recorded with BRUKER 100/S using a 1.06 μm Nd–YAG ion laser.

Results and discussion

The influence of matrix morphology on the properties of proton-conducting composites

The drastic increase of conductivity in the MJ–A composites (MJ=AgBr, TlCl, LiI, and A=Al_2O_3) was often explained in terms of the space-charge model [49, 50]. This model may be successfully applied in case of low adhesion of the salt to oxide, when heterogeneous doping induces an increase of defect concentration only in the surface layer of the ionic conductor, while it does not influence on the volume salt properties. As the interfacial interactions really define composite properties, increasing

specific surface area of the oxide components should enlarge the interface and, as a result, increase the conductivity. Such effects were observed for many systems, but are not always general in the case of highly dispersed oxides and, in particular, proton-conducting composites [51, 52]. Another important physical parameter of the oxide is its porosity (size of pores and their distribution). This was clearly shown for the composites $CsHSO_4$–SiO_2 and $RbHSO_4$–SiO_2, where the conductivity depends on the silica specific surface area if SiO_2 pore size is >10 nm, but becomes independent at the pore sizes ≤10 nm [52–56]. If SiO_2 pore size is <10 nm, practically whole salt volume confined in the pores of the highly dispersed matrix participate in the structural deformation. So, the salt amorphization becomes more energetically efficient than its surface disordering. In this case, the content of amorphous phase depends on the silica pores volume rather than specific surface area of the oxide. The decrease of the SiO_2 pores volume was shown to induce the lower conductivity value for composites based on the silica with close specific surface area S_{sp}=580–520 $m^2 g^{-1}$ (V_{por}=0.3 $cm^3 g^{-1}$, r_{por}=1.4 nm in comparison with V_{por}=0.9 $cm^3 g^{-1}$, r_{por}=3.5 nm) [52–56].

The most considerable change of the transport, structural, and thermodynamic properties was found to take place in the composites with the pore radius r_{por}=3.5–7 nm. The enthalpies of the superionic phase transition and melting of hydrosulfates exhibit the same relative changes with increasing SiO_2 content (Fig. 2), yet this change exceeds drastically the reduction of the salt mass fraction in the composites. Namely, a decrease in the salt mass fraction by merely a factor of 1.5 (x=0.7) causes the enthalpies to drop by six to seven times, indicative of a significant salt amorphization.

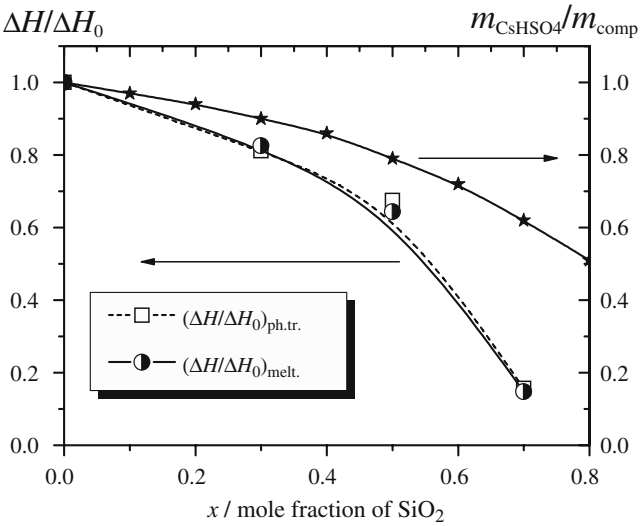

Fig. 2 The relative enthalpy of the phase transition and melting and mass fraction of $CsHSO_4$ in the $(1-x)CsHSO_4$–$xSiO_2$ composites as a function of SiO_2 content (SiO_2 specific surface area S_{sp}=300 $m^2 g^{-1}$, pore radius r_{por}=7 nm) [61]

This amorphous state provides the highest conductivity enhancement of the composite. Another disordered state of the ionic salt is observed in systems with r_{por}>10 nm. The latter corresponds to a highly dispersed state, which fraction increases with increase in the content and in the specific surface area of the oxide. A similar dependence is found for the conductivity of these composites. That state of the salt differs from the bulk one, as reflected by the temperature and enthalpy of the phase transition and melting. In fact, for such composites a variety of salt states can be stabilized, which existence was confirmed by high-resolution electron microscopy, X-ray diffraction, differential scanning calorimetry, nuclear magnetic resonance, and differential dissolution method [57]. Moreover, the conductivity depends on the composition of disordered states of the salt (amorphous and nanocrystalline) [58]; the disordered states in composites at intermediate temperatures were shown to be stable for the long time.

Consequently, in some composites not only structural disordering at the interface MJ–A, but the change of bulk properties of the ionic conductor is observed [51–60]. Evidently, the degree of structural deformation of the ionic salt depends also on the energy of surface interaction between the components and determines the transport properties of the composite.

The formation of proton-conducting composite

The hydrogen bond network as a basic attribute of solid acids make proton composite electrolytes very special among the known composite systems. It not only strongly controls the salt structure but can participate in the interfacial interaction between the components. The energy of formation of hydrogen bond is low and insignificant interface interactions can induce a sufficient change in the hydrogen bond system with following structure disordering or even amorphization of the salt, especially at high oxide content. The data of vibration spectroscopy have shown that the formation of the $CsHSO_4$–SiO_2 and $Cs_5H_3(SO_4)_4$–SiO_2 composites involve a partial sorption of salt protons by surface OH groups of silica (Fig. 3) [61–63]. The bands corresponding to the stretching and bending vibrations of the hydrogen bond net (3,600–2,000 cm^{-1}) decrease in intensity and displace to the higher frequency region. The change of intensity, displacement, splitting, and widening of the bands in the SO_4^{2-}-ions frequency region (1,200–800 and 600–400 cm^{-1} for stretching and bending vibrations, respectively) are also observed. The bands 1,000 and 1,047 cm^{-1} displace to 1,023 and 1,062 cm^{-1}, respectively. As a result, the S–O···H bonds get longer, and an increase in the symmetry of the SO_4^{2-} tetrahedrons takes place. The observed weakening of the hydrogen bonds and an increase in the orientation disorder of the HSO_4^- ions facilitates

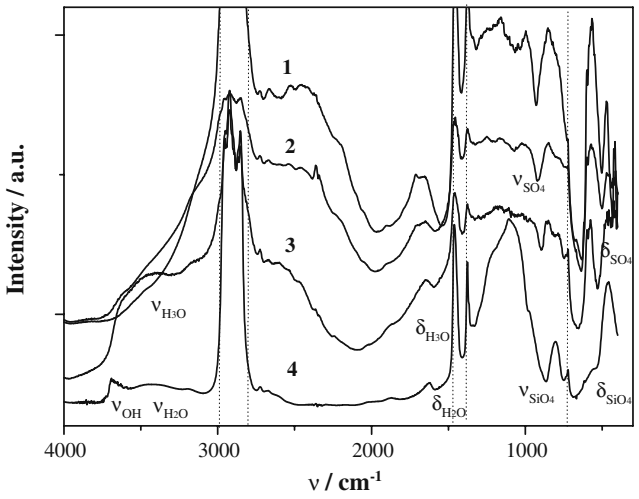

Fig. 3 IR spectra of $CsHSO_4$ and $(1-x)CsHSO_4$–$xSiO_2$ composites with different SiO_2 content: *1*—x=0, *2*—0.2, *3*—0.7, and *4*—1 (*dot lines* denote the bands of mineral oil) [61–63]

proton transport at low temperatures. The process becomes more intensive with the increase of silica content. So, the concentration of the sylanol and proton groups at the silica surface determines its acidity, which affects the salt adhesion energy and, thus, establish the degree of interfacial or chemical interaction.

The effect of acidic properties of composite components

For that reason, the acidity of oxide surface plays an important role on the composite conductivity. It was shown for composites $CsHSO_4$–A (A=SiO_2, TiO_2, Al_2O_3) that lower acidity of the oxide phase results in stronger surface interaction up to the formation of a new low-conductive phase in the systems with TiO_2 and Al_2O_3. The higher content and specific surface area of oxide was the more essential extent of new phase observed [34, 64, 65]. The systems demonstrate lower conductivity in comparison with $(1-x)CsHSO_4$–$xSiO_2$ composites, in which new phases were not obtained. All composites based on $CsHSO_4$ display the LT conductivity increase up to 1–3.5 orders of magnitude, depending on oxide content (Fig. 4). The maximal LT conductivity is observed at the oxide content of 30–50 vol.%, and then decreases due to the percolation effect "conductor–insulator." Strong surface interaction in the systems based on TiO_2 and Al_2O_3 causes a considerable decrease of the high-temperature (HT) conductivity. While $(1-x)CsHSO_4$–$xTiO_2$ composites based on modified TiO_2 with more acidic surface did not exhibit any new phases and have high and stable conductivity values at elevated temperatures [66].

Similarly, the changes in the acidic properties of the acid salts along with decrease of the cation size were found to promote interaction between the components in $(1-x)MHSO_4$–$xSiO_2$ (M=Cs, Rb, K, Na). In $(1-x)RbHSO_4$–$xSiO_2$ system slight interfacial interaction results in some texturing of the salt at the oxide surface with increase of SiO_2 mole fraction x [52, 67]. In the case of $KHSO_4$ and $NaHSO_4$, more strong interaction induces the formation of new insulating phases even at small silica content.

The influence of the salt crystalline structure and hydrogen bond network

The unusual properties were observed for the composites based on $Cs_5H_3(SO_4)_4$ yH2O containing water in the structure [61, 62, 68]. The compound has a phase transition to a high-conductive disordered state ($\sigma \sim 10^{-2}$ Scm^{-1}) at $T_{ph.tr.}$=145 °C induced by some loss of structural water. This phase transition is reversible, but the backward transformation from the HT phase is slow at the low relative humidity and can be facilitated by increasing humidity. Additional protons from the structural water improve the salt adhesion to silica. Heterogeneous doping stabilizes the highly conductive disordered state of the salt for the temperature range 100–260 °C. Not only protons from tetrahedron anions but also structural water of this salt forms hydrogen bonds with the oxide surface in the composites, so the process similar to dehydration takes place that facilitates the salt disordering and provides the composite stabilization. The temperature dependences of conductivity in some composite systems based on acid sulfates in comparison with pure salts are presented at Fig. 5.

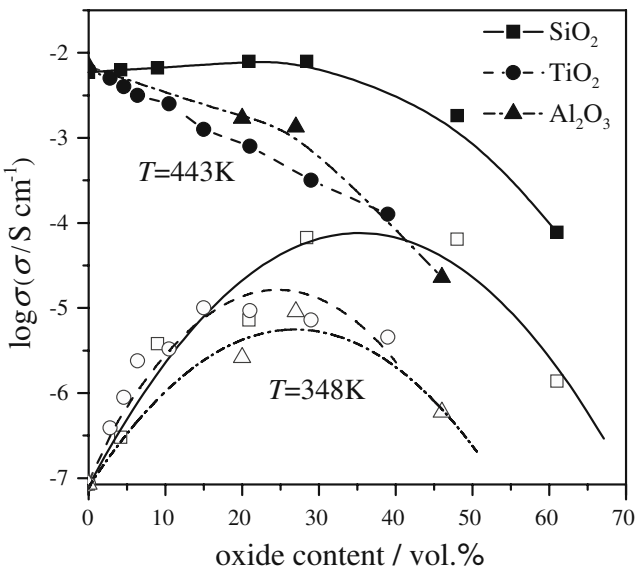

Fig. 4 The conductivity of composites $(1-x)CsHSO_4$–xA based on different oxide (A=SiO_2, TiO_2, Al_2O_3; S_{sp}=~100 m^2/g) as a function of oxide volume fraction [64, 65]

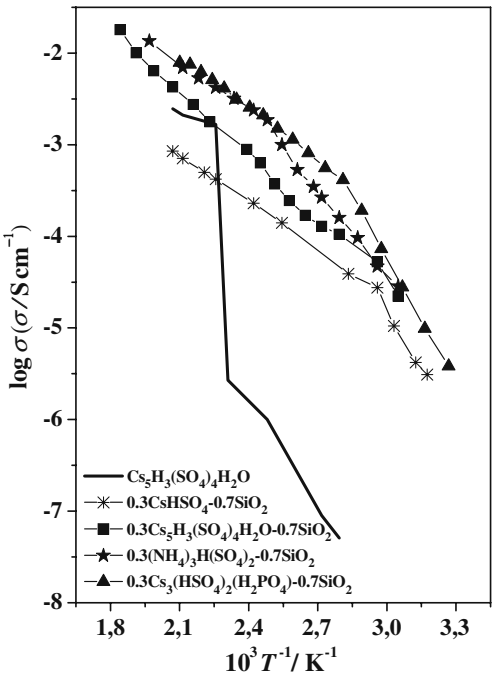

Fig. 5 Temperature dependencies of conductivity for $Cs_5H_3(SO_4)_4$ acid salt and some proton composites based on $M_mH_n(XO_4)_p$ [61, 69, 70]

Another acid salt of this family, $(NH_4)_3H(SO_4)_2$, also has additional protons from ammonium ion [19]. The compound has the crystal structure of the same type both in HT and LT polymorphs and the change of conductivity caused by the superionic phase transition is less than one order of magnitude. Heterogeneous doping by SiO_2 leads to an enhancement of the LT conductivity up to five to six times and to an insignificant decrease of the HT conductivity in comparison with polycrystalline samples (Fig. 5) [69]. At small silica content, decreasing particle size in the salt and increasing defect concentration at the interface take place. More disordered state of the salt is observed with the increase of x. Note that the thermal stability of $(NH_4)_3H(SO_4)_2$ in composites was shown to increase markedly (the temperature of decomposition increased from 387 °C up to ~437 °C), partially owing to the additional hydrogen bonds formed between protons of ammonia groups and sylanol groups of the silica surface.

Disordering in the hydrogen bond network in the acid salt facilitates its surface interaction with the oxide and following deformation of the structure, thus improving the composite conductivity. Hence, the presence of "chemically nonequivalent" oxygen atoms (in accordance with their participation in hydrogen bonding) in the mixed salt $Cs_3(HSO_4)_2H_2PO_4$ provides not only the higher proton concentration, but also superior proton mobility. The LT conductivity of $Cs_3(HSO_4)_2H_2PO_4$ is more than two orders of magnitude higher than that of $CsHSO_4$, while their conductivity values are close in the HT phases (Fig. 1) [23]. The salt with already disordered hydrogen bond network interacts easier with silica surface, in the $Cs_3(HSO_4)_2H_2PO_4$–SiO_2 composites dispergating and subsequent amorphization of the salt take place, inducing an additional increase of the conductivity. The conductivity of $(1-x)Cs_3(HSO_4)_2H_2PO_4$–$xSiO_2$ composites at x=0.7 is as high as ~10^{-4}–10^{-2} Scm^{-1}, exceeding that for $CsHSO_4$–SiO_2 system at 50–200 °C (Fig. 5) [70, 71].

In addition to the modification of fundamental properties of the acid salts in composites, another practically important parameters change due to a high energy of the salt adhesion to silica. These include, in particular, the rate of ionic salt dissolution, hydrogen permeability, mechanical strength, etc. The dissolution rate of the salt in $(1-x)CsHSO_4$–$xSiO_2$ was shown to be notably slower than that of bulk $CsHSO_4$ (up to ten times), despite the smaller particles size of the compound in composites, and to depend markedly on the composition [57]. These composites were shown to have mechanical strength three to five times higher than that of initial acid salt. Furthermore, these material have a low gas permeability (for hydrogen, <10^{-14} m^{2}c^{-1}Pa).

The peculiarities of systems based on CsH_2PO_4

Significant attention during the last years was attracted to one of the most conductive compounds in the family of acid salts—CsH_2PO_4 [72–74]. The high conductivity of CsH_2PO_4 in superionic state (6×10^{-2} Scm^{-1}) and relatively high melting point (~345 °C) make it promising for the fuel cells operating at intermediate temperatures. Really a hydrogen fuel cell based on CsH_2PO_4 membranes has already demonstrated interesting electrochemical characteristics [4, 6]. The advantages include anhydrous proton transport, an improvement of catalysts activity, an absence of noble metals, and greater tolerance to CO.

CsH_2PO_4 has a unique hydrogen bond network in which PO_4 anions are linked via O–H···O bonds at all corners of the phosphate tetrahedra, forming $[H_2(PO_4)^-]_\infty$ layers [75–77]. The structural features (in particular, the strength and dimension of hydrogen bond network) cause however a limited chemical stability of CsH_2PO_4. The range of CsH_2PO_4 superionic phase existence is limited as well: it decomposes under dry atmosphere to form $Cs_2H_2P_2O_7$ and $CsPO_3$, resulting in lower proton conductivity, while it is stable at 30 mol% H_2O vapor [78]. The narrow temperature range, the chemical instability of superionic phase, and poor mechanical properties of the crystals at high humidity are the limiting factors for its electrochemical application. Transformation of CsH_2PO_4 into more disordered systems with high conductivity at intermediate temperatures is, therefore, a very important problem.

One of the methods to modify CsH_2PO_4 transport properties is the homogeneous substitution of cesium by other ions, in particular Rb^+. The $Cs_{1-z}Rb_zH_2PO_4$ mixed salts were shown to be solid solutions up to x=0–0.9, based on CsH_2PO_4 LT structure with decreasing lattice parameters [79, 80]. The enthalpy and temperature of the superionic phase transition change with x. The proton conductivity of HT phase of $Cs_{1-z}Rb_zH_2PO_4$ is close to CsH_2PO_4 (Fig. 6). The conductivity of LT phase becomes higher with increasing of Rb^+ content.

The effect of heterogeneous dopant characteristics

The more disordered state of the salt is formed due to heterogeneous doping with dispersed SiO_2 or SiP_2O_7 [2, 44, 81–86]. The most of transport properties investigations for systems based on CsH_2PO_4 has been carried out in 30 mol% H_2O/Ar [2, 81, 82]. The comparative data on the conductivity of CsH_2PO_4 polycrystalline samples and different types of composites based on CsH_2PO_4 are shown in Fig. 7. The addition of silica (S_{sp}=~41–520 m^2g^{-1}) induces an increase in LT phase conductivity by ~0.5–1 order of magnitude, depending on temperature and silica content [44, 81, 82]. While the LT conductivity increases, the HT conductivity decreases by ~1.5–2 orders of magnitude (x=0.5) as a result of strong interface interaction. Contrary to $CsHSO_4$, the conductivity of the composites based on silica with surface acidity constant pH ~6.7–7 does not correlate with the silica specific surface area in the range S_{sp}=41–520 m^2g^{-1} [2, 44]. The data of XRD and infrared spectroscopy revealed an appearance of $Cs_2H_2P_2O_7$ phase in addition to parent CsH_2PO_4. The hydrogen bonds in

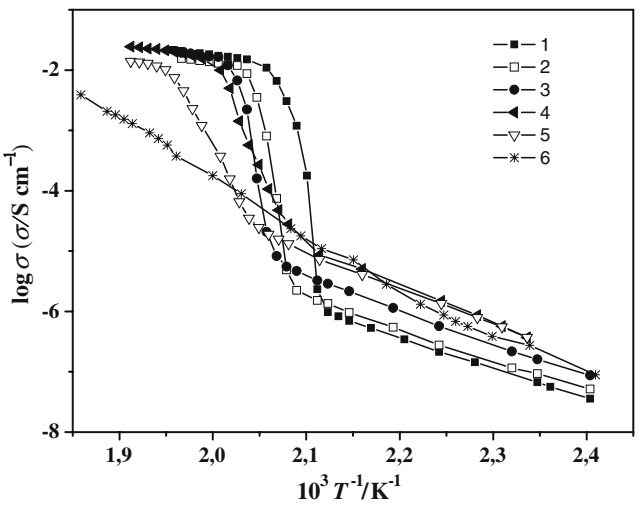

Fig. 6 Temperature dependencies of conductivity for $Cs_{1-z}Rb_zH_2PO_4$ with different Rb content: *1*—z=0, *2*—0.1, *3*—0.3, *4*—0.4, *5*—0.6, and *6*—1 [80]

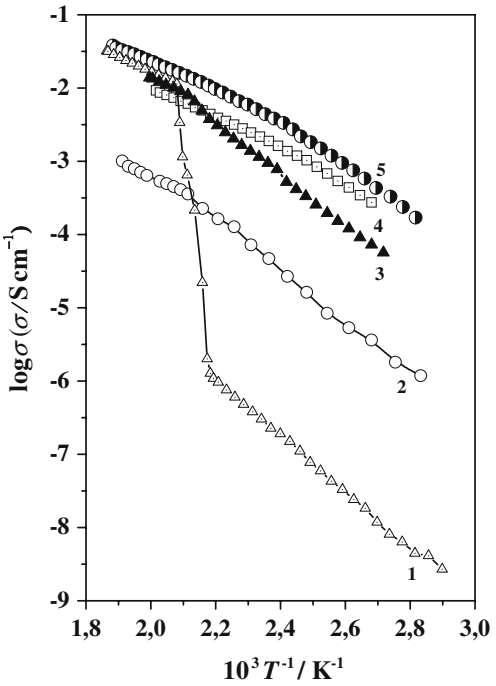

Fig. 7 Temperature dependencies of conductivity for *1* CsH_2PO_4 and CsH_2PO_4–A composites with different heterogeneous matrices A: *2*—SiO_2, *3*—SiO_2–$0.07P_2O_5$, *4*—SiP_2O_7 at 3 mol%H_2O, and *5*—SiP_2O_7 at 5 mol%H_2O [44, 83, 84]

CsH_2PO_4 are shorter, and their energy is two times higher than that of $CsHSO_4$. Unlike CsH_2PO_4 where PO_4 tetrahedrons are linked via hydrogen bonds at all corners, in $CsHSO_4$, only two oxygen atoms of the sulfate anion are hydrogen bonded forming infinite layers. Again, this results in the limited chemical stability of CsH_2PO_4 at the interface with silica.

Increasing proton concentration on the silica surface can weaken the interface interaction in the composites based on CsH_2PO_4. For these purposes, modification of silica has been carried out by the acidic additives such as H_3PO_4 or $CsHSO_4$, for which silica was shown to act as inert matrix [45, 83, 84]. These composites were shown to exhibit a high proton conductivity (~10^{-3}–10^{-2} Scm^{-1} at ~130–230 °C) due to disordered state of CsH_2PO_4 and fairly high thermal stability at lower H_2O partial pressure [45, 83, 84].

In composites with more acidic heterogeneous additive, such as SiP_2O_7 the salt amorphization was observed already at small x values as a result of interface interaction and effect of water adsorbed on matrix surface. According to DSC data, the superionic phase transition does not observed already at x=0.3. The composites also demonstrate a significant increase of the LT conductivity (more than three orders of magnitude), with maximum for x=0.3 at 3–5 mol% H_2O [45, 83–85].

The conductivity of these composites depends significantly not only on the composition, but better on humidity level. The conductivity values measured at 5 mol% H_2O/air become close for different compositions (x=0.3, 0.5, and 0.7) and the activation energy decreases from 0.8 to 0.6 eV. The temperature dependence of the conductivity for $(1-x)CsH_2PO_4$–$xSiP_2O_7$ composites deviates from Arrhenius dependence due to the presence of amorphous state of the salt and contribution of hydrated centers on the matrix surface to the overall proton transfer. The more strong chemical interaction between the components were observed under 30 mol% H_2O/Ar, resulted in the formation $CsH_5(PO_4)_2$ at the interface [2] (melting point 151.6 °C [86]) and the high proton conductivity (7×10^{-2} Scm^{-1} at 230 °C).

The heterogeneous doping by silica phosphate gels with high surface area enable a more uniform distribution of salt in the composites and also causes a significant increase of the CsH_2PO_4 LT conductivity (up to four orders of magnitude), decreasing the phase transition temperature. In these systems, the transport and thermal characteristics were shown to depend markedly not only the gel concentration but also its Si/P ratio. The silica phosphate gel composition influences on the interface interaction resulting in the stabilization of different phases. For instance, due to strong interface interaction in the systems based on SiO_2–$0.5P_2O_5$ gel [43] and SiO_2–$0.25P_2O_5$, the new compound, such as $CsH_5(PO_4)_2$ was observed limiting thermal stability of composites. While, in $(1-x)CsH_2PO_4$–x (SiO_2–$0.07P_2O_5$) composites only CsH_2PO_4 was found up to x=0.7, when its amorphization occurs. In these systems, the $CsH_5(PO_4)_2$ formation took place only at higher fractions of the matrix. Therefore, the latter systems are characterized by higher thermal stability. Contrary to pure CsH_2PO_4, the composites based on silica phosphate gel with smaller content of P_2O_5 have demonstrated high and stable conductivity values (~10^{-2} Scm^{-1}) during long-term annealing at 200 °C (400 h) at a relatively low water partial pressure (~1 mol% H_2O) in air. The dehydration of CsH_2PO_4 proceeds in two stages with the maximum weight loss equal to 7.8% (Fig. 8). Under the same conditions, the weight loss in the composite systems is lower (<2% for x=0.5), despite smaller particles size.

Thus, on the contrary to hydrosulfates, the formation of highly conductive proton composite systems based on CsH_2PO_4, transport properties, and thermal stability depend on the surface acidity of the matrix and relative humidity, in addition to all other factors discussed above. The methods of optimal modification of heterogeneous additives and CsH_2PO_4 bulk characteristics permit to obtain the systems based on SiO_2–qP_2O_5 and SiP_2O_7 with high proton conductivity (~10^{-3}–10^{-2} Scm^{-1}) at ~130–230 °C, stable at the lower humidity level as compared with the initial CsH_2PO_4.

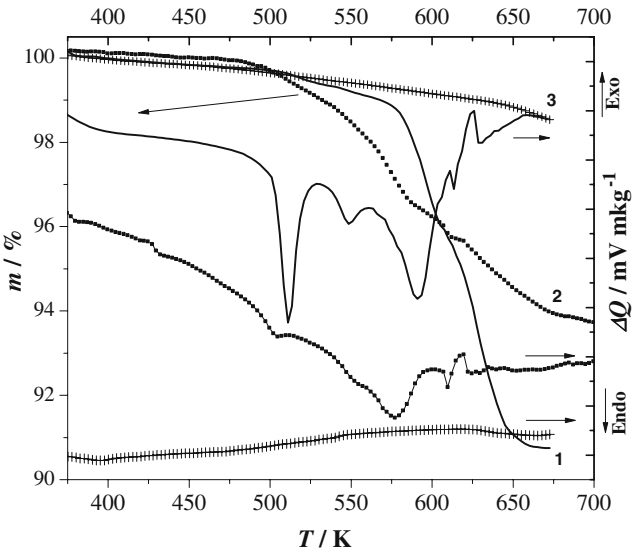

Fig. 8 DSC and thermogravimetric analysis (TGA) data for *1* CsH_2PO_4 and CsH_2PO_4–A composites with different heterogeneous matrices A: *2*—SiO_2–$0.07P_2O_5$ and *3*—SiP_2O_7 (Ar, heating rate 10 °Cmin^{-1}) [83, 84]

Besides the fast proton transport in a wide temperature range and low electron conductivity, the proton composite electrolytes based on acid salts have improved mechanical strength, low hydrogen permeability, and enhanced thermal stability at lower relative humidity. These unique properties make these systems attractive materials for application in different electrochemical devices such as: intermediate-temperature fuel cells, hydrogen sensors, separators and steam electrolyzers.

Conclusions

The systematic investigations of the composite systems based on a variety of acid salts of $M_mH_n(XO_4)_p$ family and various types of highly dispersed oxides (Al_2O_3, TiO_2, SiO_2, modified SiO_2, and SiP_2O_7) has been carried out. These composites are characterized by high conductivity values at intermediate temperatures and differed by transport, structural, and thermodynamic parameters, which in turn depends markedly on their phase composition. The type of oxide, its' morphology and pore sizes were shown to influence significantly on the structural deformation of the salt in composites. As a result, various disordered states of the salt (superionic, amorphous or nanocrystalline) are stabilized in composites, depended on their composition.

The main accent was set on structural deformation of the solid acids caused by the surface interaction of the components with the aim to distinguish the important factors determining the composite transport properties. The hydrogen bonds were shown to play an important role

in the interfacial interactions in the proton-conducting composites, which formation involves a partial sorption of the part of salt protons by the surface OH groups of the oxide. Therefore, the acid-basic properties of the oxide and its' surface, as well as the structural properties of the acid salts, especially hydrogen bond network, and cation size, have got a special interest. These central characteristics were shown to influence significantly on the energy of interface interaction up to formation of the new low-conductive phases.

Another factor determinative the salt disordering in the interface is the possibility to form additional hydrogen bonds between the components, incident to the systems based on $(NH_4)_3H(SO_4)_2$ and $Cs_5H_3(SO_4)_4\ yH_2O$. Further, the structural disordering of the initial salt, like in $Cs_3(HSO_4)_2H_2PO_4$, also facilitates the interface interaction in composites and improves considerably the proton mobility. On the contrary, CsH_2PO_4 is characterized by strong interface interaction with SiO_2 due to energetic two-dimensional hydrogen bond network. That makes easier the structural deformation of CsH_2PO_4 in the composites forward the salt dehydration at the intermediate temperatures. The additional acid centers on the silica surface were shown to decrease the interface interaction defined the thermal stability of $(1-x)CsH_2PO_4$–$x(SiO_2$–$qP_2O_5)$ and $(1-x)CsH_2PO_4$–$xSiP_2O_7$ composites at 200–230 °C. The energy of interface interaction in these systems also depends appreciably on a relative humidity.

While the energy of the interface interaction is individual value for different composite systems, however the analysis of the transport, thermodynamic, and structural properties of proton-conducting systems based on acid salts permits to modify heterogeneous additives, so as to synthesize the composite systems with high proton conductivity.

Acknowledgments This work has been carried out with a partial financial support from the Integration projects of Siberian Branch of Russian Academy of Sciences (N86 and N120).

References

1. Haile SM, Boysen DA, Chisholm CRI, Merly RB (2001) Nature 410:910–913
2. Matsui T, Kukino T, Kikuchi R, Eguchi K (2006) J Electrochem Soc 153:A339–A342
3. Haile SM, Chisholm CRI, Sasaki K, Boysen DA, Uda T (2007) Faraday Discuss 134:17–39
4. Boysen DA, Uda T, Chisholm CRI, Haile SM (2004) Science 303:68–70
5. Uda T, Boysen DA, Chisholm CRI, Haile SM (2006) Electrochem Solid State Lett 6:A261–A264
6. Uda T, Haile SM (2005) Electrochem Solid State Lett 8:A245–A246
7. Matsuo Y, Saito K, Kawashima H, Ikehata S (2004) Solid State Commun 130:411–414
8. Yoshimi S, Matsui T, Kikuchi R, Eguchi K (2008) J Power Sources 179:497–503
9. Chen X, Huang Z, Xia C (2006) Solid State Ionics 177:2413–2416
10. Matsui T, Takeshita S, Iriyama Y, Abe T, Ogumi Z (2005) J Electrochem Soc 152:A167–A170
11. Chen X, Li X, Jiang SA, Xia C, Stimming U (2006) Electrochim Acta 51:6542–6547
12. Matsui T, Kazusa N, Kato Y, Yriyama Y, Abe T, Kikuchi R, Ogumi Z (2007) J Power Sources 171:483–488
13. Baranov AI, Shuvalov LA, Schagina NM (1982) JETP Lett 36:459–462
14. Baranov AI, Merinov BV, Tregubchenko AV, Kniznichenko VP, Shuvalov LA, Schagina NM (1989) Solid State Ionics 36:279–282
15. Hainovsky NG, Hairetdinov EF (1985) Izv SO AN SSSR Ser Khim Nauk 8:33–35
16. Baranov AI, Sinitsyn VV, Vinnichenko VYu, Bonnet B, Jones DI (1997) Solid State Ionics 97:153–160
17. Baranov AI, Tregubchenko AV, Shuvalov LA, Schagina NM (1987) Sov Phys Solid State 29:1448–1951
18. Pawłowski A, Pawlaczyk Cz (1988) Ferroelectrics 81:1165–1170
19. Sinitsyn VV, Baranov AI, Ponyatovskii EG (1995) Sov Phys Solid State 37:2059–2069
20. Mhiri T, Daoud A, Colomban Ph (1991) Solid State Ionics 44:215–225
21. Mhiri T, Daoud A, Colomban Ph (1991) Solid State Ionics 44:227–234
22. Mhiri T, Daoud A, Colomban Ph (1991) Solid State Ionics 44:235–243
23. Haile SM, Lentz G, Kreuer K-D, Maier J (1995) Solid State Ionics 77:128–134
24. Haile SM, Kreuer K-D, Maier J (1995) Acta Cryst B 51:680–687
25. Haile SM, Calkins PM, Boysen D (1997) Solid State Ionics 97:145–151
26. Chisholm CRI, Haile SM (2000) Solid State Ionics 136–137:229–241
27. Liang CC (1973) J Electrochem Soc 120:1289–1298
28. Glipa X, Leloup J-M, Jones DJ, Roziere J (1997) Solid State Ionics 97:227–232
29. Uma T, Nogami M (2007) Chem Mater 19:3604–3610
30. Ponomareva VG, Burgina EB, Tarnopolsky VA, Yaroslavtsev AB (2002) Mendeleev Commun 6:223–224
31. Ponomareva VG, Tarnopol'skii VA, Yaroslavtsev AB (2006) Russ J Inorg Chem 51:343–346
32. Ponomareva VG, Tarnopol'skii VA, Burgina EB, Yaroslavtsev AB (2003) Russ J Inorg Chem 48:955–960
33. Sun C, Stimming U (2008) Electrochim Acta 53:6417–6422
34. Ponomareva VG, Uvarov NF, Lavrova GV, Hairetdinov EF (1996) Solid State Ionics 90:161–166
35. Ponomareva VG, Lavrova GV, Uvarov NF (1996) In: Chowdari BVR et al (eds) Solid state ionics: new developments. World Scientific Singapore, pp 317–322
36. Ponomareva VG, Lavrova GV, Uvarov NF (1997) In: Ramanarayanan TA et al (eds) Proc of the Third Int Symp on Ionic and Mixed Conducting Ceramics. Paris France, III, pp 44–49
37. Uvarov NF, Ponomareva VG, Lavrova GV, Brezhneva LI (2002) Mat Sci Forum 386–388:639–644
38. Tatsumisago M, Tezuka T, Hayashi A, Tadanaga K (2005) Solid State Ionics 176:2909–2912
39. Tezuka T, Tadanaga K, Hayashi A, Tatsumisago M (2006) Solid State Ionics 177:2463–2466
40. Muroyama H, Matsui T, Kikuchi R, Eguchi K (2005) Solid State Ionics 176:2467–2470
41. Diosa JE, Solis A, Vargas RA, Mellander B-E (2004) Solid State Ionics 175:459–461

42. Baranov AI, Grebenev VV, Khodan AN, Dolbinina VV, Efremova EP (2005) Solid State Ionics 176:2871–2874
43. Matsui T, Kukino T, Kikuchi R (2006) Electrochim Acta 51:3719–3723
44. Ponomareva VG, Shutova ES (2007) Russ J Electrochem 43:513–520
45. Ponomareva VG, Shutova ES (2007) Russ J Electrochem 43:521–527
46. Muroyama H, Kudo K, Matsui T, Kikuchi R, Eguchi K (2007) Solid State Ionics 178:1512–1516
47. Lavrova GV, Ponomareva VG (2008) Solid State Ionics 179:1170–1173
48. Kislitsyn M, Haile SM (2010) Chem Mater 22:2417–2426
49. Maier J (1985) J Phys Chem Solids 46:309–320
50. Agrawal RC, Gupta RK (1999) J Mater Sci 34:1131–1162
51. Chang MR-W, Shahi K, Wagner JB (1984) J Electrochem Soc 131:1213–1214
52. Ponomareva VG, Lavrova GV, Simonova LG (2000) Solid State Ionics 136–137:1279–1283
53. Ponomareva VG, Lavrova GV, Simonova LG (1998) Inorg Mater 34:1266–1269
54. Ponomareva VG, Lavrova GV, Simonova LG (1998) Inorg Mater 34:1136–1140
55. Ponomareva VG, Lavrova GV, Simonova LG (1999) Solid State Ionics 118:317–323
56. Ponomareva VG, Lavrova GV, Simonova LG (1999) Solid State Ionics 119:295–299
57. Ponomareva VG, Lavrova GV, Malakhov VV, Dovlitova LS (2006) Inorg Mater 42:1115–1120
58. Uvarov NF, Ponomareva VG, Lavrova GV (2010) Russ J Electrochem 46:772–784
59. Uvarov NF, Hairetdinov EF, Bratel NB (1993) Russ J Electrochem 29:1406–1410
60. Chen L (1986) Composite ionic conductors. In: Chowdari BVR, Radhakrishna S (eds) Composite solid electrolytes, materials for solid state batteries. World Scientific, Singapore, pp 69–75
61. Ponomareva VG, Lavrova GV, Burgina EB (2005) Russ J Electrochem 41:562–567
62. Lavrova GV, Ponomareva VG, Burgina EB (2005) Solid State Ionics 176:767–771
63. Burgina EB, Ponomareva VG, Baltahinov VP, Kostrovskiy VG (2005) J Struct Chem 46:608–618
64. Ponomareva VG, Lavrova GV (1998) Solid State Ionics 106:137–141
65. Ponomareva VG, Lavrova GV (2001) Solid State Ionics 145:197–204
66. Zencovets GA, Tsybulya SV, Burgina EB, Kryukova GN (1999) Kinet Catal 40:562–566
67. Lavrova GV, Ponomareva VG (1998) Chem Sustain Dev 6:179–182
68. Lavrova GV, Ponomareva VG (2002) Inorg Mater 38:1172–1177
69. Ponomareva VG, Merinov BV, Dolbinina VV (2001) Solid State Ionics 145:205–210
70. Ponomareva VG, Shutova ES, Matvienko AA (2004) Inorg Mater 40:721–728
71. Ponomareva VG, Shutova ES (2005) Solid State Ionics 176:2905–2909
72. Colomban Ph, Novak A (1992) Proton conductors: classification and conductivity. In: Colomban Ph (ed) Chemistry of solid state materials 2. Proton conductors. Cambridge University Press, Cambridge, p 165
73. Baranov AI, Khiznichenko VP, Sandler VA, Shuvalov LA (1988) Ferroelectrics 81:1147–1150
74. Bronowska W (2001) J Chem Phys 114:611–612
75. Sonneveld EJ, Wisser JW (1979) Acta Cryst B35:1975
76. Semmingsen D, Ellenson WD, Frazer BS, Shirane G (1977) Phys Rev Lett 38:1299
77. Uesu Y, Kobayashi J (1976) J Phys Status Solid A 34:475
78. Boysen DA, Haile SM (2003) Chem Mater 15:727–736
79. Martsinkevich VV, Ponomareva VG, Lavrova GV, Drebuschak TN, Shatskaya SS (2010) Inorg Mater 46:768–772
80. Ponomareva VG, Martsinkevich VV, Chesalov YuA (2011) Russian J Electrochem (in press)
81. Otomo J, Minagawa N, Wen CJ, Eguchi K, Takahashi H (2003) Solid State Ionics 156:357–369
82. Matsui T, Kukino T, Kikuchi R, Eguchi K (2005) Electrochem Solid State Lett 8:A256–A258
83. Ponomareva VG, Shutova ES (2007) Solid State Ionics 178:729–734
84. Ponomareva VG, Shutova ES, Lavrova GV (2008) Inorg Mater 44:1009–1014
85. Matsui T, Muroyama H, Kikuchi R, Eguchi K (2010) J Jpn Petrol Inst 53:1–11
86. Lavrova GV, Ponomareva VG (2007) Russ J Electrochem 43:454–486